Formation of magnetic nanocrystals in a glass ceramic studied by small-angle scattering

U. Lembke, A. Hoell, R. Kranold, R. Müller, W. Schüppel, G. Goerigk, R. Gilles, and A. Wiedenmann

Citation: Journal of Applied Physics **85**, 2279 (1999);
View online: https://doi.org/10.1063/1.369538
View Table of Contents: http://aip.scitation.org/toc/jap/85/4
Published by the American Institute of Physics

Formation of magnetic nanocrystals in a glass ceramic studied by small-angle scattering

U. Lembke,[a] A. Hoell, and R. Kranold
Universität Rostock, Fachbereich Physik, Universitätsplatz 3, D-18051 Rostock, Germany

R. Müller and W. Schüppel
Institut für Physikalische Hochtechnologie, Helmholtzweg 4, D-07743 Jena, Germany

G. Goerigk
Forschungszentrum Jülich GmbH, Institut für Streumethoden, D-52425 Jülich, Germany

R. Gilles and A. Wiedenmann
Hahn-Meitner-Institut, Glienicker Str. 100, D-14109 Berlin, Germany

(Received 26 June 1998; accepted for publication 17 November 1998)

The formation of nanosized crystallites of magnetite, Fe_3O_4, by heat treatment of a glass containing iron oxide was investigated. The magnetic properties of the glass ceramic manufactured strongly depend on the heat treatment conditions. The evolution of size distribution and volume fraction of the nanocrystallites formed was studied by small-angle x-ray scattering (SAXS). The size distribution of the nanocrystalline phase turned out to show bimodal shape. The possibility of magnetic contrast variation offered by small-angle neutron scattering (SANS) was utilized in order to distinguish the small-angle scattering of magnetite from the scattering contributions of nonmagnetic iron containing crystallites that can additionally be formed during the heat treatment. The results obtained reveal that both size grades of particles observed in the size distribution are superparamagnetic consisting of magnetite. The evolution of the volume fraction of magnetite in dependence on the heat treatment was found to be correlated with the magnitude of the specific saturation magnetization of the glass ceramic. The volume size distributions derived from magnetic SANS revealed peaks at smaller radii in relation to those from nuclear SANS and SAXS data. Therefore, the existence of a nonmagnetic surface layer is suggested that surrounds the magnetically active core of the magnetite nanocrystals.
[S0021-8979(99)08604-1]

I. INTRODUCTION

Nanosized spinel ferrites produced via the glass crystallization method[1] offer a new field of application due to their magnetic single domain behavior, which results in interesting magnetic properties. A unique feature of magnetite, Fe_3O_4, is its biocompatibility. It can be expected that glass ceramics containing a sufficient quantity of such ferrimagnetic nanocrystals will have manifold applications in future high frequency technology and magnetic storage devices.

In $CaO–SiO_2$ glasses with a Fe_2O_3 component, nanosized crystallites of ferrimagnetic magnetite, embedded in the nonmagnetic matrix, can be developed by a suitable heat treatment. The magnetic properties of the glass ceramic obtained are strongly influenced by the heat treatment conditions which determine the size and the volume fraction of the magnetite crystallites. Therefore, the heat treatment schedule for optimum magnetic parameters of the material has to be determined experimentally.

In combination with magnetic measurements and x-ray diffraction (XRD), small-angle x-ray scattering (SAXS) and small-angle neutron scattering (SANS) investigations can solve this problem by characterizing the size and nature of the phases formed during annealing. Owing to the magnetic moment of the neutron, SANS is sensitive not only to structural inhomogeneities but to magnetic inhomogeneities as well. Therefore, by changing the local magnetization distribution in the sample during the measurement via an external magnetic field, the magnetic scattering amplitude can be affected. This offers the opportunity to separate nuclear and magnetic scattering contributions from each other. The latter must exclusively be attributed to magnetic particles in the investigated scattering system. Consequently, by combining SAXS and SANS with varying magnetic scattering contrast more detailed information about the magnetite phase in the glass ceramic can be obtained.

II. EXPERIMENT

A. Sample characterization

The preparation of the base glass of composition 27.4 $CaO–42.8$ $SiO_2–6.1$ $B_2O_3–23.7$ Fe_2O_3 (mol %) was described elsewhere.[2] The material was investigated in the form of glassy flakes obtained by quenching the glass melt between rotating steel rollers. The initially homogeneous flakes with the density $d=3.54\ \mathrm{g\,cm^{-3}}$ were annealed in air

[a]Present address: Friedrich-Schiller-Universität Jena, Chemisch-Geowissenschaftliche Fakultät, Otto-Schott-Institut für Glaschemie, Fraunhoferstr. 6, D-07743 Jena, Germany; electronic mail: lembke@physik1.uni-rostock.de

at temperatures between 620 and 930 °C for 0.5 h up to 72 h to manufacture a magnetic glass ceramic containing nanosized magnetite crystallites.

Summarizing the previous knowledge about the glass ceramic the following main features must be mentioned:[2] The specific saturation magnetization, σ_∞, of the glass ceramic has a maximum amount of 24.4×10^{-6} V s m/kg for the heat treatment of 2 h at $T=700$ °C; both heat treatments longer than 2 h and temperatures above 700 °C lead to smaller values of σ_∞. XRD revealed that the only phase formed during the heat treatment, which can be responsible for the magnetic properties of the glass ceramic, is magnetite, Fe_3O_4. At annealing temperatures higher than 700 °C or with increasing annealing time beyond 2 h additional iron containing but nonmagnetic phases like the calcium-iron metasilicate hedenbergite, $CaFeSi_2O_6$, and hematite, Fe_2O_3, developed at the expense of the magnetite formation. From measurements of the relative saturation remanence obtained from the magnetization curve $M(H)$ for room temperature it can be concluded that up to $t=2$ h at $T=700$ °C the nanosized magnetite particles are superparamagnetic at room temperature, whereas for heat treatments at $T>700$ °C or for $t>2$ h at 700 °C the magnetite crystallites formed become larger and stable ferrimagnetic.

B. Scattering methods

The SAXS intensities were measured between $s_{\min}=0.07$ nm^{-1} and $s_{\max}=4.8$ nm^{-1} with the instrument JUSIFA at HASYLAB/DESY in Hamburg. The quantity $s=4\pi\sin(\theta/2)/\lambda$ denotes the modulus of the scattering vector $\mathbf{s}=\mathbf{k}-\mathbf{k}_0$, where $\mathbf{k}_0$ and $\mathbf{k}$ are the wave vectors of the incident and the scattered wave, respectively, and θ is the scattering angle. The x-ray wavelength $\lambda=0.177$ nm was chosen in order to avoid iron fluorescence radiation. The scattering curves recorded under these conditions contain structural information about all scattering particles in the size range between 1.4 and 45 nm. The SAXS data were background corrected and normalized to electron scattering units (e.u.) by comparing the scattering intensity of the samples with that of a calibrated glassy carbon standard. The absolute intensities, $I(s)$, measured between $s_{\min}$ and $s_{\max}$ were extrapolated to zero angle using the Sampling extrapolation formalism[3] and to infinity in accordance with the Porod law.[4]

A function, which is very suitable for assessing the structural features of a scattering system, is the correlation function $C(r)$ which is the Fourier transform of the absolute scattering intensity $I(s)$ (Ref. 5)

$$C(r)=\frac{1}{2\pi^2}\int_0^\infty I(s)s^2\frac{\sin(sr)}{sr}ds. \tag{1}$$

The absolute intensity is commonly given in electron units (e.u.) (SAXS) or barn (SANS) per unit volume, where e.u. represents the scattering intensity of a single electron, which has the dimension of a squared scattering length, and 1 barn $=10^{-24}$ cm^2 stands for the order of magnitude of the squared coherent scattering length of a neutron scattered by a nucleus. The correlation function is the averaged self-convolution of the spatial distribution of the so-called excess electron density $\Delta\rho(r)$, i.e., the difference between the local electron scattering length density and the mean electron scattering length density within the scattering sample volume. For $r=0$, the correlation function yields

$$C(0)=\langle(\Delta\rho)^2\rangle, \tag{2}$$

the mean squared electron density fluctuation, which in case of a two-phase system with homogeneous electron densities ρ_{particle} and ρ_{matrix} and the contrast $\Delta\rho=\rho_{\text{particle}}-\rho_{\text{matrix}}$ is connected with the volume fraction, w, of the particles as follows:[4]

$$\langle(\Delta\rho)^2\rangle=w(1-w)(\Delta\rho)^2. \tag{3}$$

Then, the absolute scattering intensity $I(s)$ is

$$I(s)=4\pi\int_0^\infty r^2C(r)\frac{\sin(sr)}{sr}dr. \tag{4}$$

For a homogeneous single particle, the integral in Eq. (4) yields $(\Delta\rho)^2v_p^2F_p^2(s)$, where v_p is the particle volume and $F_p(s)$ is the form factor of the particle which is normalized to unity at $s=0$. For spherical particles with a number density N_v and the differential diameter distribution function $dN(D)/dD$, which is normalized so that

$$\int_0^\infty dN(D)=N_v, \tag{5}$$

the size distribution can be calculated from the correlation function provided that interparticle interferences and multiple scattering effects are neglectable:[6]

$$\frac{\pi}{2}(\Delta\rho)^2\frac{dN(D)}{dD}=-\frac{d}{dr}\left\{\left[\frac{d^2C(r)}{dr^2}\right]\Big/ r\right\}. \tag{6}$$

Note that the size distribution obtained by Eq. (6) is weighted by the squared scattering contrast between the particles and the matrix. Both $C(r)$ and $dN(D)/dD$ can be determined from the measured scattering curve $I(s)$ by series expressions.[7]

Since the magnetic properties of the glass ceramic are very strongly connected with the volume fraction, w, of the magnetite phase the differential volume size distribution, dw/dD, is an appropriate structural function. It is calculated from $dN(D)/dD$ by weighting the size distribution with the particle volume $D^3\pi/6$ corresponding to the given size grade D. The function dw/dD obtained is normalized to the volume fraction of the particle phase, i.e., the area under dw/dD equals w.[8] Correspondingly, the integral of $dN(D)/dD$ yields the crystallite number density N_v in the sample [see Eq. (5)].

The influences of the experimental counting statistics and of termination errors due to the Fourier transform on the significance of the structure functions calculated from the scattering data were estimated according to the experiences described elsewhere.[7,9] Correspondingly, the magnitude of the errors of the correlation function $C(r)$ is comparable with the symbol size. The width of the error band of the volume size distributions dw/dD amounts to about 5%.

The SANS experiments were performed at the instrument V4 at the neutron reactor BER II of the Hahn-Meitner-

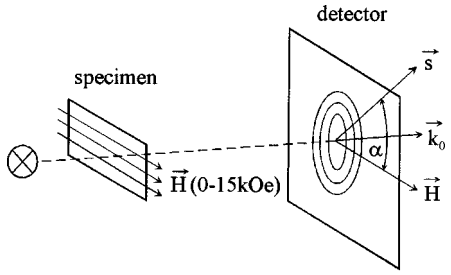

FIG. 1. Sketch of the scattering geometry.

Institute, Berlin, using a neutron wavelength of $\lambda = 0.6$ nm. The distance between the sample and the two-dimensional ^{3}He detector varied between 1.09 and 12 m covering the s range of $0.05\ \text{nm}^{-1} \leqslant s \leqslant 3\ \text{nm}^{-1}$. The SANS data were corrected concerning background scattering and absorption and were normalized to absolute scale with the help of a water standard. The overlap achieved for the SANS curves recorded with three different detector distances was excellent. The joint SANS curve was interpolated applying cubic B splines to obtain an equidistant increment, Δs.

In order to separate the magnetic scattering contribution from the nuclear scattering the sample was placed in a homogeneous magnetic field with the field strength vector, **H**, perpendicular to the direction of the primary beam as indicated in the sketch of the experimental setup given in Fig. 1. The magnetic flux density, $\mu_0|\mathbf{H}|$, was tuned up to 1 T at which the specific magnetization of the glass ceramic shows nearly saturation.[2] The scattering intensity of unpolarized neutrons varies as a function of the angle α between the external field **H** and the scattering vector **s** according to

$$I(\mathbf{s}) = A(s) + B(s)\sin^2\alpha. \tag{7}$$

If all magnetic moments are fully aligned along **H** the isotropic term $A(s)$ results solely from nuclear scattering whereas the anisotropic term $B(s)$ represents the magnetic scattering contribution only.

In the present case of superparamagnetic behavior of the nanoparticles, however, the orientation distribution of the magnetic moments **p** depends on the ratio of the energy of magnetic interaction $|\mathbf{p}||\mathbf{H}|$ to the thermal energy k_BT at the given temperature, where k_B is Boltzmann's constant. Then, the relative magnetization, $\sigma(H)/\sigma_\infty(H=\infty)$, is described by the classical Langevin function $L(x)$:

$$\sigma(H)/\sigma_\infty = L\{|\mathbf{p}||\mathbf{H}|/(k_BT)\}, \tag{8}$$

with

$$L(x) = \coth(x) - 1/x. \tag{9}$$

The modulus of the total particle moment $|\mathbf{p}|$ and hence the argument $x = |\mathbf{p}||\mathbf{H}|/(k_BT)$ depend on the diameter, D, of the particle via

$$p(D) = \frac{\pi}{6} D^3 p_{\text{Fe}_3\text{O}_4}/\Omega_{\text{Fe}_3\text{O}_4} \tag{10}$$

$$= \frac{\pi}{6} D^3 \sigma_{\infty,\text{bulk}} d_{\text{bulk}}, \tag{11}$$

where $p_{\text{Fe}_3\text{O}_4}$ and $\Omega_{\text{Fe}_3\text{O}_4}$ are the magnetic moment and the volume of one single formula unit Fe_3O_4 which can be calculated from the mass density, d_{bulk}, and the specific saturation magnetization, $\sigma_{\infty,\text{bulk}}$, of bulk magnetite, Fe_3O_4.

For noninteracting single-domain particles embedded in a nonmagnetic matrix, it was shown that the anisotropic part $B(s)$ has a completely magnetic origin:[10]

$$B(s) = \{1 - 3L(x)/x\} m^2(s), \tag{12}$$

whereas the isotropic part $A(s)$ contains the nuclear scattering amplitude, $n(s)$, and the magnetic scattering amplitude, $m(s)$, as well:

$$A(s) = n^2(s) + 2L(x)/x\, m^2(s). \tag{13}$$

The functions $n(s)$ and $m(s)$ are the Fourier transforms of the nuclear and magnetic neutron scattering length densities, respectively.

It should be noted that for strong external fields and sufficiently large particle dimensions $A(s)$ represents essentially the nuclear scattering contribution, since the magnetic part proportional to $2L(x)/x$ vanishes for large x values as does the factor $3L(x)/x$ in Eq. (12) [see Eqs. (8)–(11)]. Therefore, in that case the magnetic scattering contribution $m^2(s)$ can be obtained from $B(s)$ and the nuclear scattering $n^2(s)$ is expressed by $A(s)$, when the two-dimensional SANS pattern is analyzed according to Eq. (7). However, the condition of a negligible value of $L(x)/x$ is not fulfilled for very small sizes of the magnetic particles. Consequently, the effect of the Langevin factors in Eqs. (12) and (13) have to be considered in the further evaluation of the scattering data. In particular, this problem leads to the disadvantage that, corresponding to Eq. (13), the nuclear scattering information contained in $A(s)$ is superimposed by magnetic scattering contributions if very small magnetic particles exist. Under these conditions, the scattering curve for zero field $I(s, H=0)$ should preferably be used as nuclear scattering contribution instead of $A(s)$.

The calculation of structural parameters and functions from the SANS curves $A(s)$, $B(s)$, and $I(s, H=0)$ is analogous to the procedure described in the case of SAXS intensities if the nuclear and magnetic neutron scattering length densities $\Delta\eta_{\text{nuc}}$ and $\Delta\eta_{\text{mag}}$, respectively, are used instead of the electron density $\Delta\rho$ in Eqs. (2)–(6):

$$\Delta\eta_{\text{nuc}} = N_A \left(d_{\text{particle}}/M_{\text{particle}} \sum_i c_i b_i - d_{\text{matrix}}/M_{\text{matrix}} \sum_j c_j b_j \right) \tag{14}$$

and

$$\Delta\eta_{\text{mag}} = b_{\text{mag}} \sigma_{\infty,\text{bulk}} d_{\text{bulk}}, \tag{15}$$

where c and b stand for the mole fractions and the nuclear scattering lengths of the atomic species in the particle (i) or the matrix (j). The mass densities of the phases are given by d; M is the molar weight of the corresponding phase and N_A is Avogadro's number. The quantity $b_{\text{mag}} = 0.27 \times 10^{-12}$ cm/μ_B is the magnetic scattering length per Bohr magneton, $\mu_B = 1.165 \times 10^{-29}$ V s m.

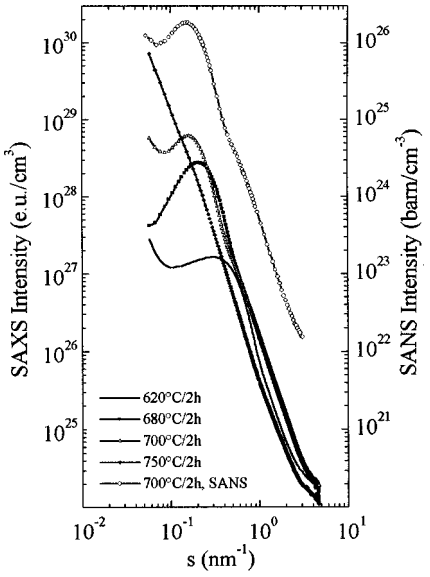

FIG. 2. SAXS and SANS curves extracted from the isotropic two-dimensional scattering patterns by radial integration and normalized to absolute scattering units. The SAXS intensity distributions were obtained from samples heat treated for 2 h at the indicated temperatures. The SANS curve was registered for the sample heat treated for 2 h at 700 °C with $\mathbf{H}=0$.

III. RESULTS AND DISCUSSION

The evolution of the phases crystallizing in the base glass during different stages of heat treatment is demonstrated by the corresponding SAXS curves in Fig. 2. Obviously, the 2 h heat treatments with temperatures increasing from 620 up to 700 °C lead to growing volume fractions and particle sizes of the developing microcrystalline phase. This is indicated by the rising SAXS intensities at intermediate *s*-values and a shift of the SAXS curve to smaller *s*-values with increasing temperature.

As revealed by XRD,[2] the SAXS effect observed for samples heated at $T\leqslant 700\,^{\circ}\mathrm{C}$ should mainly be caused by the magnetite crystallites formed. However, for annealing times $t>2$ h at $T=700\,^{\circ}\mathrm{C}$ or for heat treatments at higher temperatures the SAXS effect, which is typical for the magnetite crystal phase, diminishes in favor of a very strong scattering intensity at small *s* values. The latter arises from particles essentially larger than the magnetite crystallites. These particles are assigned to nonmagnetic crystalline phases containing iron, the volume fractions of which increase at the expense of the magnetite phase. This interpretation is consistent with the observed decrease of the specific saturation magnetization of the glass ceramic manufactured under these conditions. The corresponding XRD results[2] give evidence of the formation of iron metasilicate-like phases and hematite (α-Fe_2O_3).

Based on the assumption that the only phase crystallized for $T\leqslant 700\,^{\circ}\mathrm{C}$ should be magnetite quantitative evaluation of the SAS data recorded is possible. The correlation functions, $C(r)$, calculated from the SAXS curves, $I(s)$, presented in Fig. 2 are shown in Fig. 3. The volume fractions, *w*, of the magnetite crystallites in the samples were determined from $C(0)$ according to Eqs. (2) and (3) using the contrast $\Delta\rho=\rho_{\mathrm{magnetite}}-\rho_{\mathrm{matrix}}$ given by the known compositions and

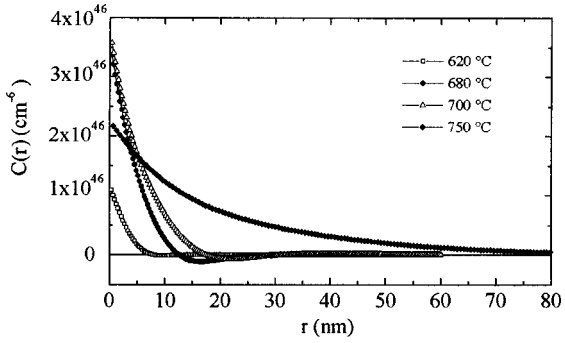

FIG. 3. Correlation functions calculated according to Eq. (1) from the SAXS curves shown in Fig. 2.

mass densities of the two phases. The values of *w* obtained are compared with the measured specific saturation magnetization, σ_∞, of the glass ceramic in Fig. 4. It becomes obvious that maximum saturation magnetization is achieved for treatment conditions which supply the maximum volume fraction, $w_{\max}$, of magnetite. The value of $w_{\max}=18.0\%$ extracted for the SAXS data is within the limits which might be expected from a rough estimation based on the relation of the magnitude of σ_∞ of the glass ceramic to the saturation magnetization of bulk magnetite. In case of the sample heat treated at $T=750\,^{\circ}\mathrm{C}$, the proportionality between σ_∞ and *w* suggested for the lower treatment stages is apparently distorted. This effect comes from nonmagnetic phases, which are formed at 750 °C in addition to the magnetite nanocrystals,[2] and leads to a calculated value of the volume fraction which is higher than the real magnetite phase volume *w*.

As can already be deduced from the correlation maxima of $I(s)$ in Fig. 2, the shape of the $C(r)$ curves gives a hint on interparticle interference effects as well. This is indicated by the course of $C(r)$ below the abscissa at large *r* values (Fig. 3). The shape of $C(r)$ in this region is caused by a superposition of the correlation function of the dilute particle system, which should have the value $C(r)\equiv 0$ for $r\geqslant D_{\max}$ with

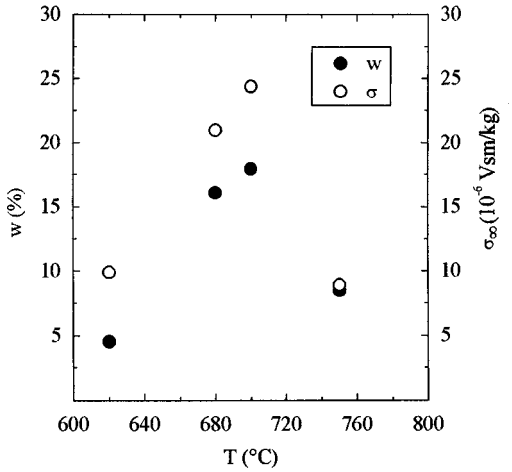

FIG. 4. Magnetite volume fraction, *w*, and the specific saturation magnetization, σ_∞, of the glass ceramic manufactured vs heat treatment temperature; treatment time $t=2$ h.

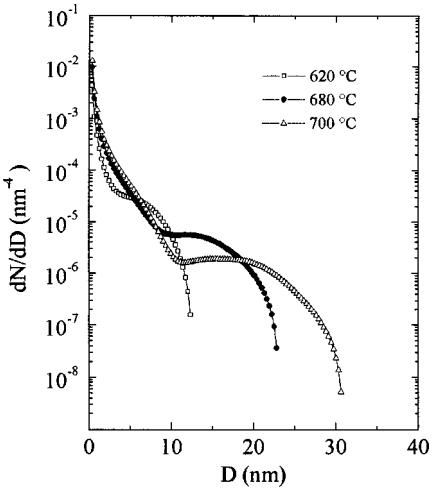

FIG. 5. Differential particle size distributions calculated from the SAXS data in Fig. 2.

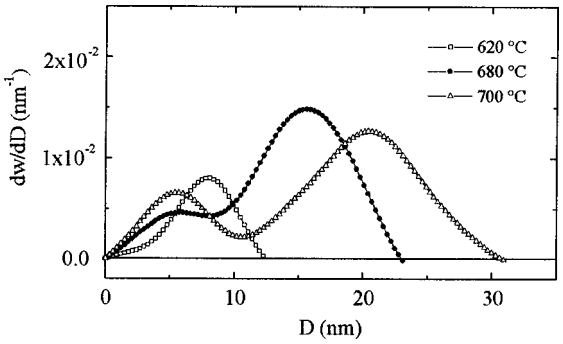

FIG. 6. Differential volume size distributions dw/dD obtained using the data shown in Fig. 5. The integral of dw/dD is normalized to the phase volume, w, of the magnetite nanocrystals.

$D_{\max}$ representing the diameter of the largest particle in the scattering system, and long range correlations of the closely packed particles.[11] However, the interparticle interference effect in $C(r)$ is not pronounced and $D_{\max}$ can be well approximated by the position of the minimum in $C(r)$. The values obtained confirm that, according to the Sampling theorem, the angular resolution of the SAS experiments performed was sufficiently high to guarantee maximum structural information about the investigated particle systems for all samples treated at $T \leqslant 700\,^{\circ}\mathrm{C}$.[12] Moreover, the shape of $C(r)$ for $r < D_{\max}$ is only marginally affected by the interparticle interference effect.

The latter conclusions are of great importance for authorizing the calculation of size distributions from the SAS patterns. As already mentioned, the results obtained for dN/dD and, consequently, dw/dD by means of Eq. (6) are exact only in that case that the scattering particles are homogeneous spheres in a dilute system, i.e., for $1-w \approx 1$. Whereas the condition of a spherical shape is fulfilled, as has been proved by transmission electron microscopy (TEM),[2] the influence of the dense packing of the particles cannot fully be neglected. Nevertheless, interparticle interferences should be of secondary importance for the calculation of the size distributions according to Eq. (6) in the present case. Thus, the size distributions determined should represent quite reasonable estimates of the exact structural functions.

The magnetite size distributions obtained from the SAXS data shown in Fig. 2 are given in Fig. 5. Owing to the very high number density of the small magnetite crystallites a logarithmic scale was useful. The shape of the size distribution dN/dD points out that a population of very small particles exists, the number of which exceeds by about three orders of magnitude the number of the large crystallites. As already mentioned, the magnetic properties of the glass ceramic depend on the volume fraction w of the crystallites. Therefore, the differential volume size distributions, dw/dD, shown in Fig. 6 are appropriate to study the evolution of the crystallite size and phase volume in dependence on the heat treatment conditions. According to the growing phase volume of magnetite the area under dw/dD increases with increasing treatment temperatures up to $T = 700\,^{\circ}\mathrm{C}$. The volume size distributions change from an unimodal shape at 620 °C to a bimodal shape at higher treatment temperatures. Obviously, the appearance of the sort of very small magnetite crystallites is not pronounced for the treatment at 620 °C for 2 h or their mean size is smaller than the resolution limit of the SAXS experiment.

The existence of bimodal size distributions is a phenomenon well known for phase separating or crystallizing glasses. This type of size distribution can develop if so-called athermal nuclei, which have been formed by homogeneous nucleation during quenching of the melt down to room temperature, and/or a limited number of heterogeneous nucleation sites exist when the isothermal heat treatment begins. Then, the present nuclei immediately start growing, whereas, at the same time, the homogeneous nucleation of additional magnetite crystallites is delayed by the so-called nucleation time lag.[13,14] Consequently, under these circumstances, two generations of particles of the same phase can develop which have well distinguishable mean dimensions. Another scenario that can lead to bimodal-type size distributions does not need the suggestion of heterogeneous or athermal nuclei, but is based on homogeneous nucleation and diffusion-limited growth only. As revealed by model computations for the silver halide precipitation in a sodium borate glass, a bimodality of the size distribution can be obtained if a size-dependent effective diffusion coefficient in consequence of elastic strain effects is taken into account.[14] This behavior is typical for phase formation processes in viscoelastic systems which are characterized by a difference of several orders of magnitude between the diffusion coefficient of highly mobile monomers forming the new phase and that of the viscous matrix phase.

Turning to the results of the SANS experiments it is important to remark that the two-dimensional SANS pattern of the sample annealed at 700 °C for 2 h measured at zero external field was found to be completely isotropic. This behavior is expected for random orientation of the superparamagnetic moments. By azimuthally averaging the isotropic two-dimensional SANS pattern, the curve drawn in Fig. 2 was obtained which is practically identical with that of the corresponding SAXS curve.

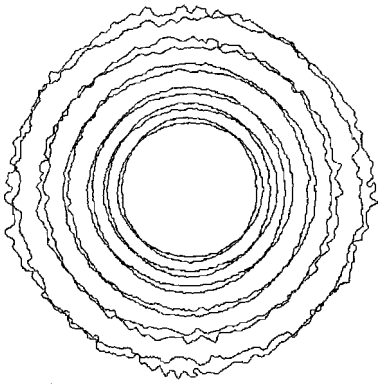

FIG. 7. SANS pattern recorded with $\mu_0|\mathbf{H}|=1$ T for the sample heat treated at 700 °C/2 h. The iso-intensity contours of the pattern are drawn twice but rotated to each other by 90° in order to demonstrate their anisotropy.

An anisotropic two-dimensional SANS pattern is expected if the magnetic moments within the crystallites are aligned along an external homogeneous magnetic field. This behavior was significantly observed for the same sample (700 °C, 2 h) at $\mu_0|\mathbf{H}|=1$ T. In Fig. 7, a deviation of the scattering pattern from radial symmetry becomes evident when the measured pattern is rotated by 90°. Therefore, Eq. (7) can be used to separate the isotropic and anisotropic scattering terms which are shown in Fig. 8. As clearly can be seen $I(s,H=0)$, $A(s)$ and $B(s)$ reveal a similar shape of the intensity distribution, but $B(s)$ is shifted to somewhat larger s values. The shoulder visible in the tails of all scattering functions shown refer to a sort of particles essentially smaller than the crystals responsible for the main scattering effect. The low level of $B(s)$ indicates a very small magnetic contrast of the magnetite nanocrystals relative to the nonmagnetic matrix.

In Fig. 9, the volume distribution is presented which has been calculated from $B(s)$ and which corresponds to the magnetic scattering term of the sample heat treated at 700 °C for 2 h. According to Eq. (12), the anisotropic scattering $B(s)$ shown in Fig. 8 is influenced by a factor depending on

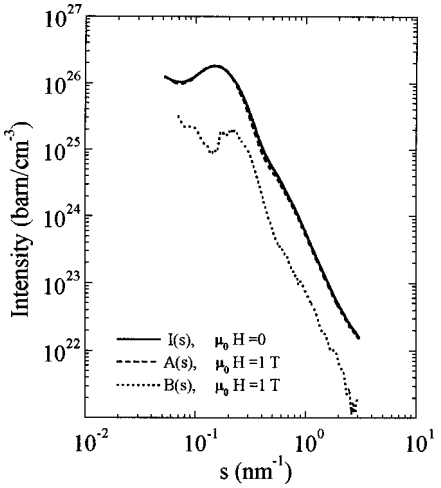

FIG. 8. Comparison of the scattering curves of SANS with $\mathbf{H}=0$, and the isotropic, $A(s)$, and the anisotropic, $B(s)$, SANS contributions separated according to Eq. (7) from the pattern shown in Fig. 7.

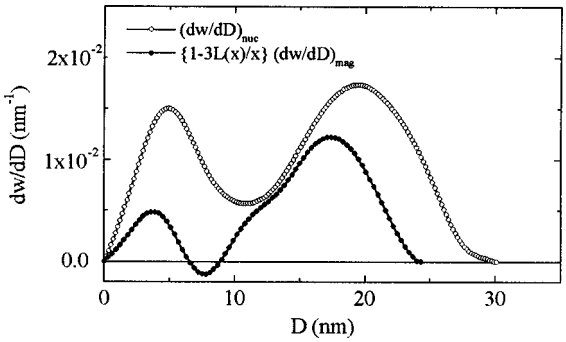

FIG. 9. Volume size distributions vs crystallite diameter D obtained from SANS for $\mathbf{H}=0$ [nuclear scattering $n^2(s)$] as well as from the anisotropic scattering function $B(s)$ in Fig. 8 by correcting the functions dw/dD for the corresponding scattering contrasts. The function $(dw/dD)_{\mathrm{mag}}$ represents that fraction of particles the magnetic moment of which can be aligned by the external magnetic field. Heat treatment: 700 °C, 2 h.

the Langevin function $L(x)$. Consequently, the differential size distribution calculated from $B(s)$ according to Eq. (6) and also the corresponding volume size distribution are weighted by the factor

$$[1-3L(x)/x](\Delta\eta_{\mathrm{mag}})^2\pi/2, \tag{16}$$

where $\Delta\eta_{\mathrm{mag}}$ is the magnetic scattering contrast of magnetite, Fe_3O_4, relative to the non-magnetic matrix. Corresponding to Eq. (15), the value of $\Delta\eta_{\mathrm{mag}}=1.357\times10^{10}$ cm^{-2} can be calculated from the specific saturation magnetization $\sigma_{\infty,\mathrm{bulk}}=1.13\times10^{-4}$ V s m/kg and the mass density $d_{\mathrm{bulk}}=5.18$ g/cm^3 of bulk magnetite, Fe_3O_4. In Fig. 9, the factor $(\Delta\eta_{\mathrm{mag}})^2\pi/2$ was removed from the differential volume size distribution calculated from $B(s)$. Therefore, the remaining distribution $[1-3L(x)/x](dw/dD)_{\mathrm{mag}}$ represents the volume size distribution of those fractions of the magnetite particles which can be magnetized by the external magnetic field $\mathbf{H}$.

Additionally, in Fig. 9 the volume size distribution $(dw/dD)_{\mathrm{nuc}}$ of the same sample is drawn which has been obtained from the nuclear scattering, i.e., SANS for $\mathbf{H}=0$. According to Eq. (14), the nuclear scattering contrast used in Eq. (6) was estimated to $\Delta\eta_{\mathrm{nuc}}=2.166\times10^{10}$ cm^{-2}. Obviously, the shapes of dw/dD obtained from the nuclear scattering as well as from the magnetic scattering are very similar in both cases. Their bimodal kind indicates the fact that not only the large particles but also the second particle population with essentially smaller mean size must consist of magnetite. This qualitative conclusion is very important and obtainable exclusively with the help of neutron scattering, since SAXS is not sensitive to the magnetic contrast existing in the magnetic glass ceramic investigated. Moreover, due to the very low dimension of the smallest sort of magnetite crystallites, XRD experiments are not able to analyze their composition.

Another very important conclusion can be drawn from the results shown in Fig. 9. The function $[1-3L(x)/x]\times(dw/dD)_{\mathrm{mag}}$, corresponding to the magnetic scattering contribution, reflects apparently smaller crystallite sizes than $(dw/dD)_{\mathrm{nuc}}$. At first sight this behavior seems to depend on the prefactor $[1-3L(x)/x]$ which describes the influence of

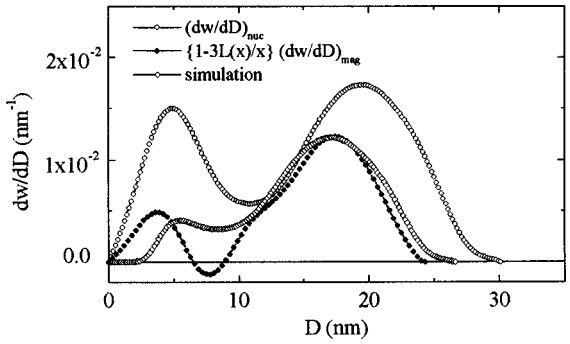

FIG. 10. Comparison of the volume size distributions obtained from (a) the nuclear scattering (SANS for $\mathbf{H}=0$), from (b) the anisotropic scattering term $B(s)$, and (c) by simulating the effect of a nonmagnetic surface layer with the double thickness $\Delta D = a \cdot D + b$. Heat treatment: 700 °C, 2 h.

the size of the magnetite nanocrystals on their magnetization. However, using the data of Fe_3O_4 and Eqs. (8)–(11) it can be estimated that the factor $[1-3L(x)/x]$ is approximately unity for $D>7$ nm.

Consequently, at least for the sort of large particles the shift between the volume distributions in Fig. 9 cannot be explained by the effect of the Langevin factor $[1-3L(x)/x]$, i.e., the superparamagnetic behavior of the nanocrystals. The shift of dw/dD rather suggests the presence of a nonmagnetic surface layer[15] around the nanosized magnetite crystallites. As can be estimated from the mean diameters of the respective dw/dD peaks for the larger crystallites in Fig. 9, the magnetically active crystallite core is 19% smaller than the size of the whole crystallite. The mean thickness of the non-magnetic layer should amount to 1.3 nm for the sort of larger magnetite crystallites, as determined from the shift of the corresponding peak of dw/dD in Fig. 9.

The dimension of the nonmagnetic layer located on the surface of the magnetite crystallites can be further investigated by model calculations. This can be performed by shifting the function dN/dD obtained from the nuclear SANS scattering ($\mathbf{H}=0$) by the double shell thickness, $\Delta D = \Delta D(D)$, along the D axis just conserving the total number of particles with sizes $D>\Delta D(0)$. This results in the model size distribution $dN(D^*)/dD^*$, with $D^*=D-\Delta D(D)$, which subsequently is transformed into the corresponding model volume size distribution $dw(D^*)/dD^*$. Afterwards, this function is multiplied with the prefactor $[1-3L(x)/x]$, where x depends on D^* now. This procedure simulates the apparent crystallite shrinkage effect and even the loss of very small crystallites for the magnetic scattering term which should be caused by such nonmagnetic surface layers. Best agreement of the simulated volume size distribution with $\{1-3L(x)/x\}(dw/dD)_{\mathrm{mag}}$ is obtained assuming $\Delta D(D) = a \cdot D + b$ with $a=0.082$ and $b=1.0$ nm. In Fig. 10, the simulated distribution is compared with the experimentally observed distribution. It must be emphasized that a constant surface layer thickness or a fit for $b=0$ do not reasonably match to the measured volume size distribution of the magnetic scattering contribution.

The structural meaning of the term b in the model function of the double shell thickness, $\Delta D = \Delta D(D)$, should consist in a lower limit for the crystallite dimension of magnetite below which the exchange interaction of the magnetic ions is distorted to such an extent that no long range ordering persists in the magnetite particle. This might be happening due to a structural distortion of the periodic lattice for extremely small particles. As the fit result $b=1.0$ nm is in the order of the edge length of the spinel unit cell of magnetite (0.8 nm), it can be concluded that, to a first approximation, magnetite particles do not show a definite crystalline (magnetic) structure until they contain more than one single spinel unit cell with 8 Fe_3O_4 units. Consequently, on the one hand, for large magnetite crystallites $b/2$ should contain that part of the nonmagnetic layer thickness which is due to the distorted crystalline structure of the surface region and results in a correspondingly distorted magnetic structure. On the other hand, the value of $b/2$ can be influenced by a thermically induced reduction of the exchange field between the ionic magnetic moments in the crystallite surface relative to that inside the particles.[15]

The dependence of the nonmagnetic layer thickness on the size of the magnetite crystallites according to $a \cdot D$ is a very unexpected result. As a possible reason the oxidation of Fe_3O_4 on the surface of the magnetite particles can be discussed. An oxygen content slightly higher than that of Fe_3O_4 can destroy the magnetic order within the magnetite unit cell. The suggestion of an oxidation shell formation is consistent with the development of hematite, Fe_2O_3, for a treatment duration longer than 2 h at 700 °C which is going on at the expense of the magnetite phase volume.[2] Hematite is antiferromagnetic with a negligible magnetic moment. The proportionality between the thickness of the oxidation shell on the crystallite surface and the size of the magnetite nanocrystals cannot reasonably be explained up to now. Nevertheless, it is obvious that the shell thickness and the radius of the magnetite particles grow according to the same temperature dependence.

IV. CONCLUSIONS

The evolution of nanosized magnetite crystallites in a glass ceramic was investigated for different heat treatment conditions. The SAXS results obtained reveal that the size distributions of the crystallites formed have bimodal shape. The sensitivity of SANS to heterogeneities of the magnetization density allowed experiments with variation of the magnetic contrast of the magnetite nanocrystals in relation to the matrix phase. The results obtained by this method show that both sorts of crystallites, which can be distinguished by distinct mean sizes in the bimodal size distributions, must be attributed to magnetite. The magnetite volume fraction extracted from the scattering data turned out to be proportional to the specific saturation magnetization of the glass ceramics manufactured under different conditions of heat treatment. The anisotropic magnetic scattering term, which contributed to the SANS pattern of the glass ceramic in an external magnetic field, was analyzed in terms of a superparamagnetic behavior of the nanosized magnetite particles. The existence of a non-magnetic surface layer around the magnetite nanocrystals was indicated by an apparent shrinkage of the crystallites which was deduced from the volume size distribu-

tions obtained from the magnetic scattering term. By model calculations, the thickness of the surface layer turned out to depend on the size of the magnetite nanocrystals. Consequently, magnetic contrast variation by SANS is a tool to measure directly the thickness of these interface regions by comparing the size distributions obtained from the nuclear and magnetic scattering contributions.

ACKNOWLEDGMENT

The authors gratefully acknowledge the financial support of the Deutsche Forschungsgemeinschaft (INK 6).

[1] R. Muller and W. Schüppel, J. Magn. Magn. Mater. **155**, 110 (1996).
[2] A. Hoell, R. Kranold, U. Lembke, R. Brückner, R. Müller, P. Görnert, and W. Schüppel, Ber. Bunsenges. Phys. Chem. **100**, 1646 (1996).
[3] G. Damaschun, J. J. Müller, and H.-V. Pürschel, Acta Crystallogr., Sect. C: Cryst. Struct. Commun. **27**, 11 (1971).
[4] G. Porod, Kolloid-Z. **124**, 83 (1951).
[5] L. A. Feigin and D. I. Svergun, in *Structure Analysis by Small-Angle X-Ray and Neutron Scattering*, edited by G. W. Taylor (Plenum, New York and London, 1987).
[6] J. H. Letcher and P. W. Schmidt, J. Appl. Phys. **37**, 649 (1966).
[7] G. Walter, R. Kranold, T. Gerber, J. Baldrian, and M. Steinhart, J. Appl. Crystallogr. **18**, 205 (1985).
[8] U. Lembke, K. Grosse, R. Pascova, I. Gutzow, O. Becker, and L. Horn, J. Mater. Sci. **31**, 4333 (1996).
[9] U. Lembke and T. Gerber, J. Appl. Crystallogr. **18**, 55 (1985).
[10] J. Kohlbrecher, A. Wiedenmann, and H. Wollenberger, Z. Phys. B **104**, 1 (1997).
[11] G. R. Strobl, M. J. Schneider, and I. G. Voigt-Martin, J. Polym. Sci., Polym. Phys. Ed. **18**, 1361 (1980).
[12] T. Gerber and P. W. Schmidt, J. Appl. Crystallogr. **16**, 581 (1983).
[13] I. Gutzow, Contemp. Phys. **21**, 121 (1980); **21**, 243 (1980).
[14] J. Bartels, U. Lembke, R. Pascova, J. Schmelzer, and I. Gutzow, J. Non-Cryst. Solids **136**, 181 (1991).
[15] S. Kurisu, T. Ido, and H. Yokoyama, IEEE Trans. Magn. **23**, 3137 (1987).